THE ASTROPHYSICAL JOURNAL, 389:590–601, 1992 April 20

MODELING OF THE ECLIPSING BINARIES IN THE GLOBULAR CLUSTER NGC 5466[1]

J. KALLRATH
Astronomische Institute der Universität Bonn, Auf dem Hügel 71, 1D-5300 Bonn, Germany
AND
E. F. MILONE AND C. R. STAGG
Rothney Astrophysical Observatory, University of Calgary, 2500 University Drive, NW, Calgary, AB, Canada 72N 1N4
Received 1991 March 21; accepted 1991 October 29

ABSTRACT

The discovery of three eclipsing binaries in the globular cluster NGC 5466 (Mateo et al.) is a boon to studies of both this ancient (18 Gy) cluster and close binaries. Two of the systems discovered by Mateo et al. appear to be contact systems and one appears to be a short-period Algol system. Basic parameters, especially the masses, of the stars in these systems are urgently required for the evaluation of the binary merger hypothesis for the origin of blue stragglers, and as a test of cluster evolution models. Here we present the results of a study of viable models of these interesting systems, based on a simplex-enhanced, Kurucz-atmospheres version of the Wilson-Devinney Program. The simplex enhancement goes further than our WD version in that it optimizes automatically all four spot parameters of one spot on the cooler star; as far as we know, this is the first time this has been carried out with the simplex treatment. This procedure was necessary to model the O'Connell effect in two of these systems. The resulting parameters are more or less consistent with the expected properties of the stars and of the cluster.

Subject headings: binaries: eclipsing — globular clusters: individual (NGC 5466)

1. INTRODUCTION

Contact systems are rare in globular clusters and also in very young open clusters; indeed, there are few binaries known in globular clusters at all. This is unfortunate because eclipsing, double-lined spectroscopic binaries provide the means for the direct determination of the masses of distant stars. Masses of stars at known positions on the color-magnitude diagram provide extremely important checks on cluster model ages and chemical composition. Moreover, the rarity of binaries in globulars argues for a mechanism that evolves detached binaries into contact systems and ultimately into blue stragglers, which tend to be less rare in old and intermediate age open clusters, for example, than in younger clusters. The connection between W UMa stars and blue stragglers has recently been discussed by Eggen & Iben (1989) and by Mateo et al. (1990), while angular momentum loss through magnetic field braking, the likely mechanism for the evolution, has been discussed by Mochnacki (1981), Rahunen (1981), and by Guinan & Bradstreet (1988). The metamorphic origin for contact systems, albeit by less-efficient gravitational radiation, had been suggested also by Webbink (1976). Since merged, spun-down stars must be the ultimate end-product of angular momentum loss, the hypothesis seems to account qualitatively for the observations. The discovery by Mateo et al. (1990) of three eclipsing systems in NGC 5466 ($14^h05^m.0$, $+28°34'$, 1990.5) provides an opportunity to determine the properties of the systems at specific stages of their metamorphoses.

The objects of interest are NH 19, 30, and 31 using the Nemec & Harris (1987) designations. Their basic properties as given in Mateo et al. (1990) are listed in Table 1. Mateo et al. (1990) provide V and partial B passband light curves of all three objects.

NH 31 has an Algol-like light curve which displays only modest curvature at maximum light as well as a substantial secondary minimum and therefore could be a detached system. If so, it presents a possible standard candle and probe for evolution studies (see Milone & Schiller 1988, 1990 and references given therein for discussions of the value of eclipsing binaries for such purposes). Its significance for binary star evolution is underscored by its period: at just over $0^d.5$, it may be the shortest period Algol system detected to date.

NH 19 and NH 30 appear to be contact systems on the basis of light curve shape. The contact systems show depth differences and NH 19 shows a clear O'Connell effect (difference between the maxima); we have demonstrated that spot modeling sufficies as a treatment of the asymmetries, and to that end have undertaken analyses with our improved version of the Wilson-Devinney program (see Milone et al. 1991; Milone, Stagg, & Kurucz 1992) which includes spot-modeling and a new atmospheres option, and with a simplex-enfolding version developed by JK.[2] The latter, to be discussed elsewhere, permits the extensive exploration of parameter space and thus places limits on the ranges of possible solutions.

2. PHOTOMETRIC ANALYSIS PROCEDURES

For each binary we began with the preliminary elements derived by Mateo et al. (1990). The initial input data were entered into DC (Differential Corrections subroutine) input files and tested for-self consistency with the University of Calgary's enhanced Wilson-Devinney (hereafter WD) code on the Cyber 205 supercomputer and the Myrias SPS-2 64-processor computer. Initial values for log g (needed for the WD program atmospheres option), the surface potentials, and the monochromatic luminosity, L_1 (subscript 1 refers to the

[1] Publications of the Rothney Astrophysical Observatory, No. 60.

[2] Initials, when not otherwise identified, refer to one of the authors, here Josef Kallrath.

TABLE 1

ECLIPSING BINARIES IN NGC 5466

Object	mag (V)	$B-V$	P
NH 31	18.8–19.1	0.15	$0^d.511230$ (4)
NH 19	18.4–18.7	0.15	$0^d.342144$ (6)
NH 30	19.2–19.6	0.15	$0^d.297536$ (6)

component eclipsed at phase $0^p.0$), were enlightened guesses, and the latter two quantities were modified as required by DC. For each of the three systems, the temperature and mass of the hotter star were fixed at the temperatures derived by Mateo et al. from observed $B-V$ color indices applied to Schmidt-Kaler's (1982) tables for Population II stars of metallicity [Fe/H] ≈ -2.0. The limb-darkening coefficients, $x_{1,2}$ were obtained from the tables of Wade & Rucinski (1985); bolometric albedoes were fixed at 1.0, based on the relatively early spectral types assumed for all stars in the study; the values for x_2 were initially set equal to x_1 and were altered when T_2 was obtained from the earliest trials. Although limb darkening coefficients of contact system components are usually taken equal, the improved WD program permits different values of x_2 in mode 3 (for contact systems).

Following the initial DC runs, the data files were downloaded to the Z-386 microcomputer of the Astronomy Data Reduction Lab at the University of Calgary, incorporated into the input file of a newly created simplex-enhancement of the University of Calgary's version of the WD program (hereafter SWD). The fixed values of input data for each system are provided in Table 2; these include the effective temperature (T_1) averaged over the surface of the hotter star, designated as star 1. The simplex algorithm was first employed for eclipsing binary analyses by Kallrath (1987) and Kallrath & Linnell (1987) and has been subsequently used by Breinhorst et al. (1989), Drechsel et al. (1989), and by Walker & Chambliss (1990). For a further review of simplex usage for light curve analysis, see Kallrath (1992). Our enhancement was tested on the systems AI Phe (Milone, Stagg, & Kurucz 1992) and TY Boo (Milone et al. 1991), a detached and contact system, respectively, and was found to yield minima in parameter space identical to those obtained by the nonautomatic iterations performed with the WD code, within the probable errors of the determined parameters. Spot optimization for all four spot parameters required by the WD code was included in the enhancement. Consequently, the simplex-enhanced program was felt to be an ideal tool to probe the ranges of solutions for the binaries discovered by Mateo et al. We will describe this program (Kallrath 1992) and demonstrate its power for delineating solutions of still other systems (Milone et al. 1991, 1992; Stagg et al. 1992; Schiller et al. 1992; Nelson et al. 1992) elsewhere; at present it suffices to say that it has all the enhancements of our WD code but has been modified further to permit spot parameters to be optimized automatically for a spot, on the second (usually cooler) component. To our knowledge, this is the first time spot parameters have been modeled under the simplex regime of operations. Systems NH 19 and NH 30 both required the input of a spot because of large O'Connell effects in these systems, and one spot proved sufficient in these cases. This code (as well as the WD version previously used for AI Phe and TY Boo analyses) has been ported to the Sun 4 and SPARCstation platforms of the Image Processing and Astronomy Data Reduction Laboratories and uploaded to the University of Calgary's IBM RISC RS6000 320 workstations in the university's Academic Computer Centre from a Zenith 386 microprocessor, on which SWD was developed.

The data given by Mateo et al. (1990) for these faint stars have large scatter and are fairly sparse, especially within the minima. Because of the latter condition, we found it necessary to weight data at minimum light with up to 10 times the weight of data at maximum light in order to obtain an initial solution which does justice to the minima. The difficulty is common to all least-squares problems in which there are heavily unequally distributed data points with equal weights assigned to each of them. The solution will be insensitive to sparsely populated but structurally important regions of the light curve. Once a solution which successfully fits the sparsely populated regions is found, the weights of these points may be made equal without affecting the final solution parameter set. The use of nonzero values of the Wilson-Devinney *noise* parameter (permitting application of additional weights proportional either to the inverse of the light level, or to the inverse of the square of the light level) did not substantially improve the fitting process in preliminary trials and was set to 0 for all the formal trials described below. Following the main series of trials, and starting from the final values, we subjected the DC fittings to additional DC trials (although the same results could have been

TABLE 2

FIXED MODELING PARAMETERS

	NH 31				
	Transit				
PARAMETER	Detached	Semidetached	Occultation	NH 19	NH 30
$a(R_\odot)$	2.85	2.85	2.85	2.18	1.99
e	0.00	0.00	0.00	0.00	0.00
$F_1 = F_2$	1	1	1	1	1
$g_1 = g_2$	1	1	1	1	1
$A_1 = A_2$	1	1	1	1	1
T_1 (K)	8410	8410	9429	8200	8130
$x_1(V)$	0.488	0.488	0.434	0.468	0.461
$x_2(V)$	0.504	0.504	0.494	0.468	0.461
$x_1(B)$	0.592	0.592	0.523	0.549	0.534
$x_2(B)$	0.584	0.584	0.607	0.549	0.534
l_3	0	0	0	0	0
ω	90°	90°	90°	90°	90°

expected with Simplex, too), this time with equal weighting for each datum. The results of these final trials, which were effectively unchanged, will be discussed for each system at the end of §§ 3–4.

The ranges of the variables of the adjustable parameters were fixed to physically realizable extremes ($\leq 90°$ for i, etc.). Initially, the simplex was configured to cover a substantial part of parameter space and was checked, before iteration, to ensure that the values of each adjusted variable fell within ranges compatible with the physics of the WD program and with reasonable expectations of the component stars. After adjustments, the program was run with sufficient numbers of iterations to achieve the desired precision. The figure of merit used by the program is the standard deviation of the fit as provided by the residuals between the observed and computed light curves.[3] In each case the simplices were run on either the IBM RS6000 540 compute server or a 320 workstation. Each run was halted when either the volume of the simplex decreased below a stipulated low limit or the number of iterations reached a given value (see Kallrath & Linnell 1987, p. 356, for a fuller discussion of termination criteria). For all stars, the geometry was *not* fixed in advance; in *each* case, analysis was begun in the WD mode 2, appropriate for detached stars. For NH 19 and NH 30, the system quickly converged to the contact system, and subsequent trials were run in the WD mode 3, appropriate for contact systems. We now describe the modeling of each system in turn, beginning with NH 31.

3. NH 31

From its published light curve (Mateo et al. 1990), NH 31 appeared to be a detached system; if it were so, the extent to which the components evolved can test theoretical isochrones predicted for NGC 5466. The system shows a slight O'Connell effect, but we did not attempt to model spot parameters to account for it during these trials, unlike those for NH 19 and NH 30, where the effect is much greater.

The temperature of star 1, eclipsed at primary minimum, was fixed at $T_1 = 8410$ K, as per Mateo et al. Atmospheres for both components were assumed to be radiative, so that gravity darkening coefficients $g_1 = g_2$ were assumed to be 1.0. The atmospheres mode with $\log g = 4.5$ for both components was used for all trials.

The SWD solutions of the varied parameters for five representative solutions out of a large number of trials are given in Table 3. In this and subsequent tables, N is the number of simplex iterations. The inclination was adjusted in early trials but always moved to $i = 90°$, and was subsequently fixed at this value.

As noted by Mateo et al., two sets of solutions are possible: the *transit* case, where the hotter star eclipsed at primary minimum is the larger star, and is thus transited by its smaller, cooler companion; and the *occultation* case, where the hotter star is the smaller, and is occulted by the larger, cooler star at primary minimum. The sizes of the stars were not directly constrained in the trials we conducted of these two cases. Instead, the mass ratios were constrained so that the "transit" case is, in essence, the result of constraining q to be <1, and in the "occultation" case to be >1. Since the relative potentials of the stars are dependent on the mass ratio, and since the physics of the modeling assumes that stars fill their potential surfaces, this is a nearly equivalent constraint for the present system.

[3] The standard error of the fit in this context is defined by

$$\sigma_{\rm fit} = \sqrt{[\Sigma w_i (l_i^o - l_i^c)^2]} \cdot \sqrt{\{[n/(n-m)]/\Sigma w_i\}} ,$$

where n and m are the numbers of data points and free parameters respectively, l^o and l^c are the observed and computed light, respectively, and w is the weight of an observation.

TABLE 3

NH 31 SIMPLEX-DERIVED PARAMETERS: TRANSIT CASE

Parameter	S1	S2	S3	S4	S5
Mode	2	2	2	2	5
Ω_1	3.418	3.417	3.318	3.318	3.073
Ω_2	2.901	2.899	3.035	3.035	2.474
q	0.386	0.386	0.478	0.477	0.304
T_2 (K)	7175	7175	7360	7360	7309
L_1 (V)	8.67	8.67	8.66	8.66	8.82
L_1 (B)	...	8.67	9.18	9.20	9.30
σ	±0.046	±0.046	±0.040	±0.040	±0.038
N	85	63	110	66	81

The first set of trials involved the case of a transit at primary minimum. As we noted above, the initial mass ratio was assumed to be less than one for this case. The properties of the intermediate and final SWD models are described in detail below:

Solution set S1 is the result of a run with all weights for the sparse B light curve set equal to zero;

S2 is the result of restarting the simplex at S1;

S3 is the solution including the B light curve data;

S4 is nearly identical to S3 and is the result of restarting the simplex process at the final parameter configuration of S3. S3 and S4 clearly represent a deep minimum in six-dimensional parameter space; and, finally,

S5 is the result of modeling in the Wilson-Devinney mode 5 in which a semidetached configuration, with star 2 filling its inner lobe, is assumed.

Explorations of other areas of parameter space for the case $q < 1$, yielded worse fittings, as gauged by the appearance of the V light curve and by the formal error.

Consequently, we adopted S4 and S5 as equally likely potential solutions for the transit case. These solutions were then entered as input into the University of Calgary version of the non-simplex Wilson-Devinney code. This is a necessary step to obtain the uncertainties in the adjusted quantities, and it permits a check on the minimizing procedure used in SWD. In most cases, the differential corrections technique suggested small changes. This is to be expected because the simplex code works on *all* adjusted parameters, not on subsets. Nevertheless, within two or three iterations, the best fit of the uncorrelated subsets of adjusted parameters was achieved, confirming that the simplex code did indeed identify the deepest multidimensional minimum of parameter space under the constraints of the parameter variations. The final DC parameters are shown in Table 4, which contains, in addition to the probable errors of the full set of adjusted quantities, the radii of the components. The agreement between observed and the S4 and S5 sets of computed light curves is seen in Figures 1*a* and 1*b*, respectively. Although redundant and not included here, the residual plots to check for systematic deviations were made and examined; they are available on request. The B light curve is so sparse that it serves only as a rough check on the determinations, which are surprisingly good considering the scatter in

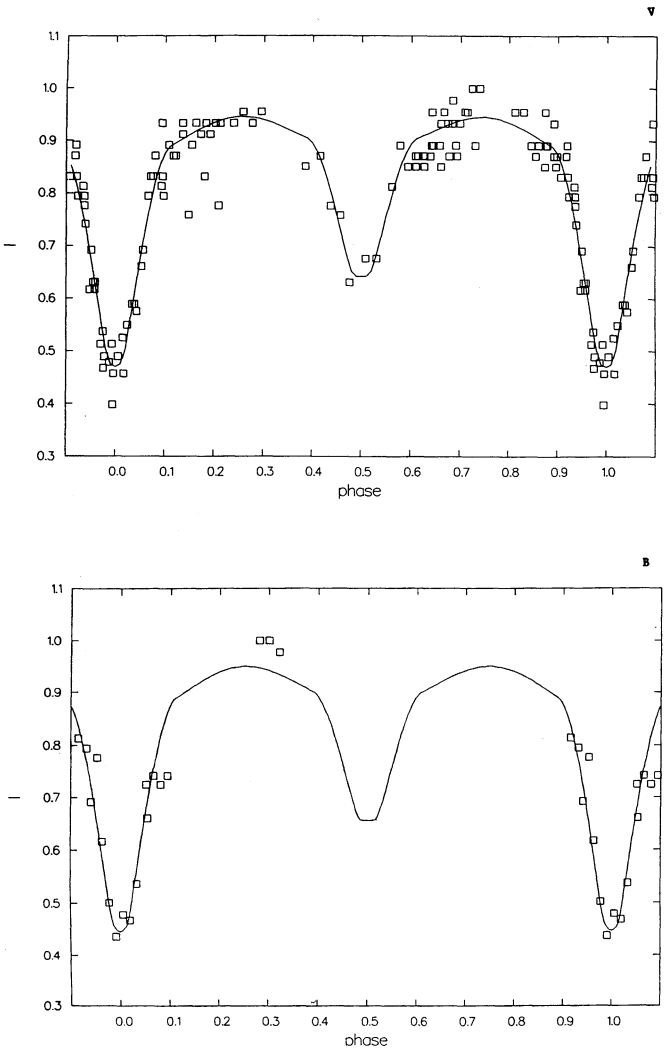

FIG. 1*a*

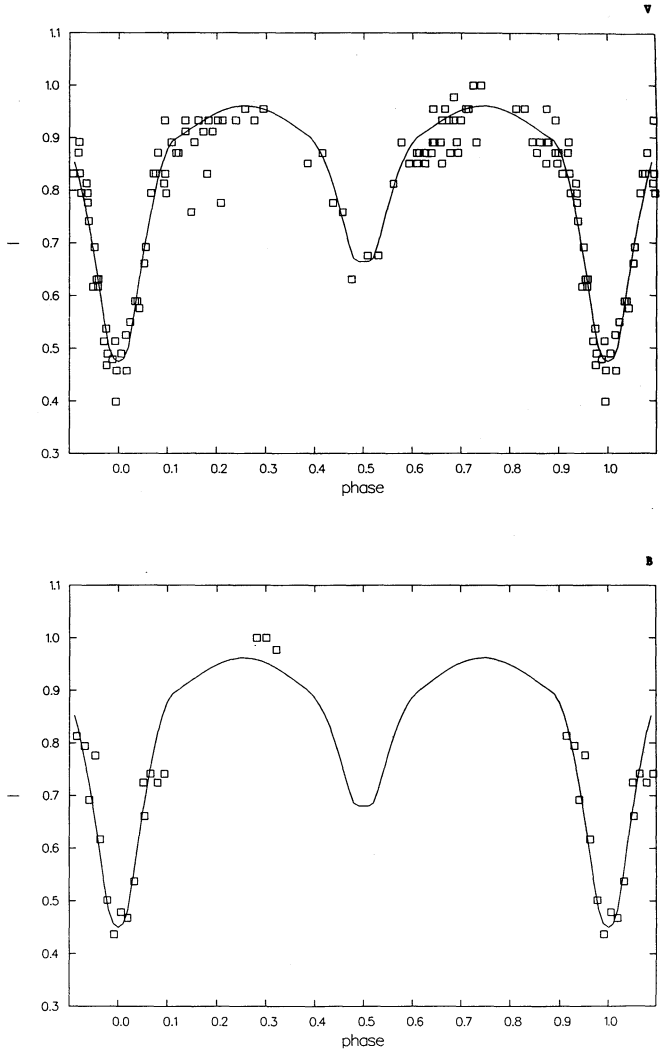

FIG. 1*b*

FIG. 1.—Observed data and computed V and B light curves of the detached, transit (*a*) and semidetached transit (*b*) and occultation (*c*) models (Table 4) of the system NH 31 in the globular cluster NGC 5466.

the light curves. As expected, the mass ratio, q, is not well constrained by the present light curves alone; the modeling for the transit case indicates the presence of a trough in parameter space between mass ratios between 0.3 and 0.5.

The case of occultation at primary minimum was also explored, i.e., the case $q > 1$ was considered. The temperature assumed for T_1 was taken as 9429 K, as per Mateo et al. (1990). The Wilson-Devinney run converged in a few iterations to the configuration shown in Table 4. The initial potential values (Ω_1 and Ω_2) were started at values close to their Roche lobes; convergence carried them to large values (corresponding to smaller radii) immediately so that the semidetached option was not viable in this case. However, to be sure that another, deeper minimum of parameter space did not lie beyond a peak or ridge in this direction, SWD was again run with initial parameters equal to the final DC values, but with looser constraints on the adjusted parameters, including sizes. The results are shown for this case in the last column of Table 3. The residuals are slightly greater in the occultation case (Σwr^2 in Table 4) compared to the semidetached so that this model is slightly less preferred to that of the semidetached transit case. Especially notable is that the secondary minimum is predicted to be deeper than the few observations indicate (see Fig. 1*c*); but more data are needed to decide the validity of this model.

Following all the trials discussed in this section, new sets of trials were carried out with DC on the V and B light curves in which now each datum was assigned equal weight. The results are not significantly different, although the uncertainties are slightly changed; they are shown in the lower half of Table 4. The altering of the weights produced large changes in the quantity Σwr^2 for each model, which should be used to compare solutions for similarly weighted light curves only. The basic conclusions are unaltered in that the semidetached transit solution appears to be the favored model, based on current data and constraints.

The x-z plane profile of the system in each of the three adopted preliminary solutions (upper half of Table 4) is shown in Figure 2, which show also the inner and outer Lagrangian surfaces, and the resulting dimensions and scale of the system. Should Figure. 2*a* or 2*c* more accurately reflect the physical state of the system, the stars are contained within the inner Lagrangian surfaces. Such a state would be a necessary

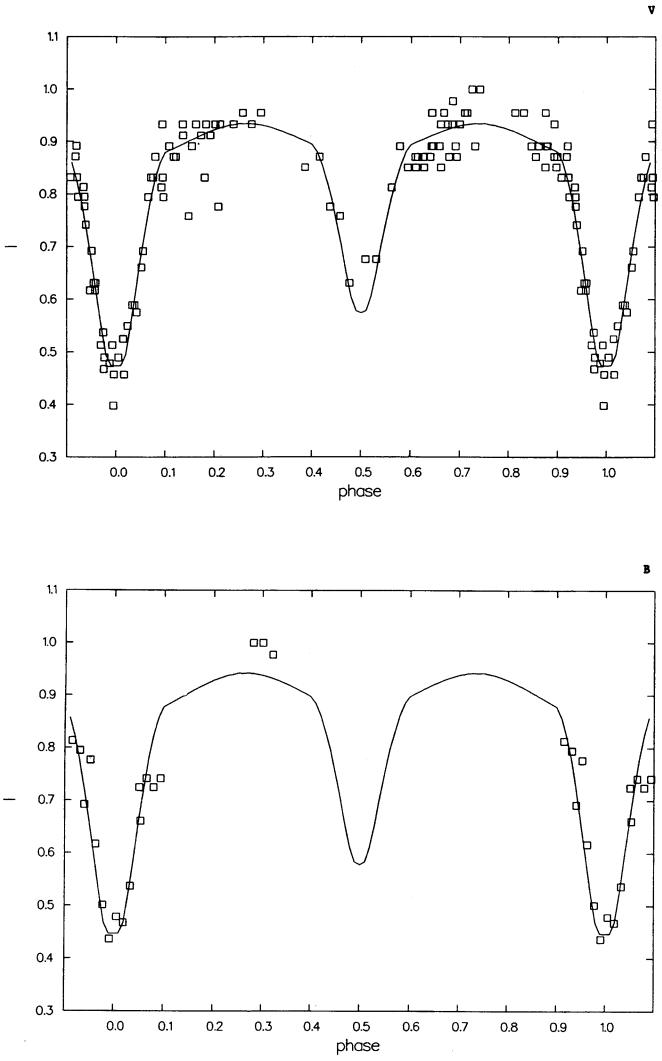

FIG. 1c

although perhaps not sufficient condition for them to be probes of the evolutionary state of NGC 5466, assuming they are contemporary with other stars of the cluster and not products of a more recent cluster merger or star burst episode. It would be a sufficient condition if evolutionary path calculations were to show that neither star could have filled its Roche lobe previously, as Schiller & Milone (1988) demonstrate for the detached system in NGC 752, DS Andromedae. That condition certainly cannot be assumed given the proximity of the stars to their Roche lobes in these preliminary solutions, and the circumstance that the semi-detached solution is slightly favored. Further model improvement and informed evolutionary discussion cannot proceed effectively, in our view, until the masses of these components are known or higher precision light curves for these faint objects can be obtained.

We have not explored the effects of altering T_1 beyond what was initially assumed by Mateo et al. for both transit and occultation cases, and await spectroscopic data to improve on those values. The light ratio L_1/L_2 in the transit case for B is $\sim$3.5, and in V is $\sim$3.0; for the occultation case, L_2 is slightly more luminous: $L_1/L_2 \approx 0.8$ in B and 0.7 in V. In both cases, L_1/L_2 values are sufficiently small to permit double-line detection at reasonable signal to noise at moderately high resolution.

TABLE 4

NH 31 FINAL DC PARAMETERS

PARAMETER	TRANSIT		OCCULTATION
	Detached	Semidetached	
Unequally Weighted Minimum Solutions			
i	90°	90°	90°
Ω_1	3.318 ± 0.040	3.082 ± 0.036	5.351 ± 0.107
Ω_2	3.003 ± 0.054	2.405[a]	5.000 ± 0.108
q	0.456 ± 0.016	0.273 ± 0.023	1.488 ± 0.047
T_2 (K)	7330 ± 85	7309 ± 80	8465 ± 66
$L_1(V)$	8.691 ± 0.162	8.816 ± 0.138	4.957 ± 0.134
$L_1(B)(4\pi)$	9.021 ± 0.252	9.132 ± 0.226	5.230 ± 0.156
$L_2(V)(4\pi)$	2.918	2.917	6.813
$L_2(B)(4\pi)$	2.615	2.616	6.573
R_1/a (pole)	0.346 ± 0.004	0.354 ± 0.005	0.256 ± 0.006
R_1/a (point)	0.377 ± 0.006	0.376 ± 0.008	0.277 ± 0.008
R_1/a (side)	0.358 ± 0.005	0.365 ± 0.006	0.261 ± 0.006
R_1/a (back)	0.368 ± 0.005	0.371 ± 0.007	0.271 ± 0.007
R_2/a (pole)	0.259 ± 0.005	0.254 ± 0.006	0.346 ± 0.007
R_2/a (point)	0.296 ± 0.008	0.370 ± 0.008	0.391 ± 0.012
R_2/a (side)	0.266 ± 0.005	0.265 ± 0.006	0.359 ± 0.008
R_2/a (back)	0.283 ± 0.007	0.297 ± 0.006	0.375 ± 0.009
Σwr^2	2.909	2.881	3.059
σ	0.0384	0.0382	0.0393
Equally Weighted Minimum Solutions			
i	90°	90°	90°
Ω_1	3.321 ± 0.053	3.082 ± 0.043	5.399 ± 0.102
Ω_2	3.026 ± 0.052	2.341[a]	5.000 ± 0.140
q	0.456 ± 0.016	0.245 ± 0.014	1.488 ± 0.047
T_2 (K)	7274 ± 133	7370 ± 132	8453 ± 87
$L_1(V)(4\pi)$	8.741 ± 0.236	8.662 ± 0.199	4.957 ± 0.146
$L_1(B)(4\pi)$	9.157 ± 0.284	9.026 ± 0.251	5.230 ± 0.163
$L_2(V)(4\pi)$	2.767	2.858	6.524
$L_2(B)(4\pi)$	2.483	2.599	6.285
R_1/a (pole)	0.346 ± 0.005	0.351 ± 0.004	0.247 ± 0.006
R_1/a (point)	0.376 ± 0.008	0.371 ± 0.005	0.264 ± 0.008
R_1/a (side)	0.357 ± 0.006	0.361 ± 0.005	0.252 ± 0.006
R_1/a (back)	0.368 ± 0.007	0.366 ± 0.005	0.260 ± 0.007
R_2/a (pole)	0.255 ± 0.004	0.247 ± 0.004	0.328 ± 0.008
R_2/a (point)	0.290 ± 0.005	0.360 ± 0.005	0.364 ± 0.011
R_2/a (side)	0.263 ± 0.004	0.257 ± 0.004	0.339 ± 0.009
R_2/a (back)	0.278 ± 0.005	0.289 ± 0.004	0.353 ± 0.010
Σwr^2	0.241	0.235	0.256
σ	0.0408	0.0403	0.0421

[a] Fixed at the inner Lagrangian surface potential.

4. NH 19

NH 19 was initially interesting because the difference in depths (0.15 mag), O'Connell effect, and possible occultation secondary, suggested it to be candidate for an A-type W UMa system in the broken contact phase of thermal relaxation oscillations. Work to date does suggest that $0.4 < q < 0.5$, with a slight preference for values close to 0.5, so that it appears to be an A-type system; however, as we will show, the system is almost certainly overcontact, so that this scenario is inappropriate. Radiative atmospheric albedoes (1.0), and gravity darkening coefficients were adopted for this relatively early-type system. M_{tot} was fixed at 1.2 $M_\odot$ and T_1 was fixed at 8200 K. The fixed parameters are listed in Table 2. The early trials of this system suggested that the minima were not well-centered about zero phase; accordingly, the *phase* variable in both the

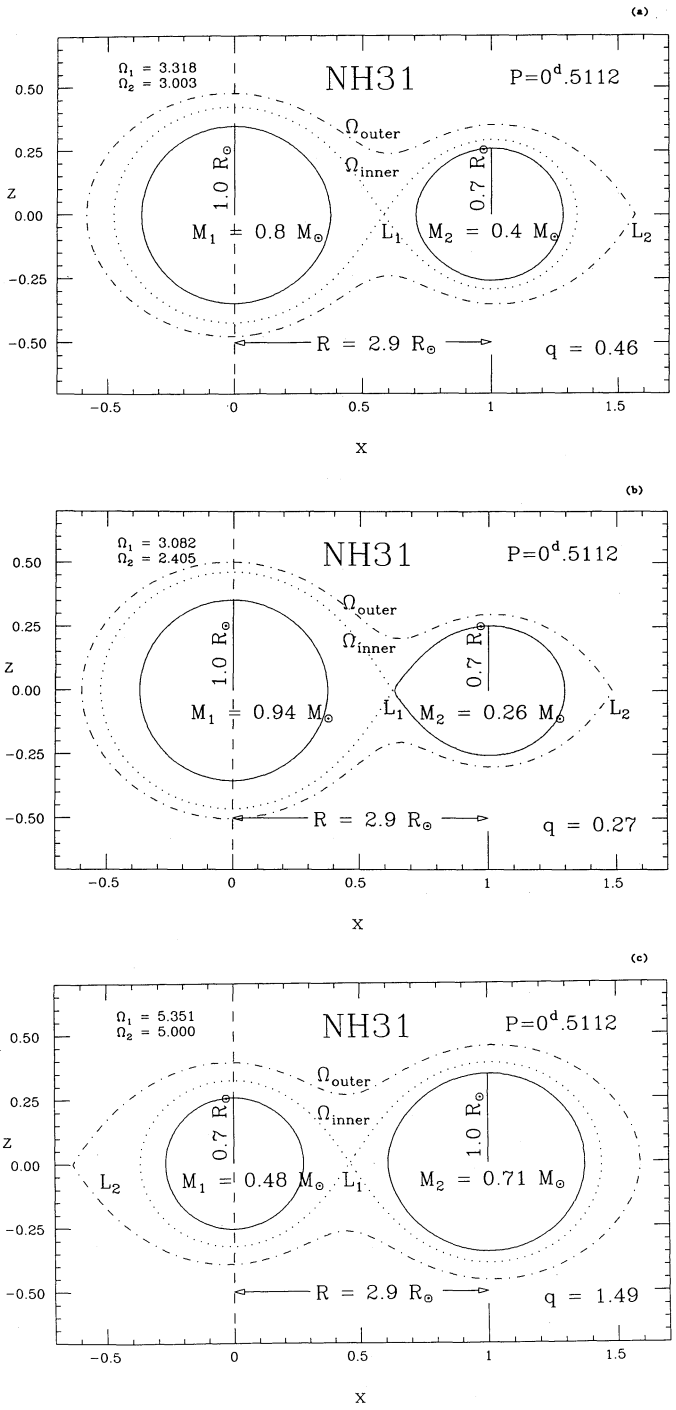

FIG. 2.—The x-z plane profile of the short-period Algol system NH 31 in each of the two adopted preliminary solutions for the transit case (detached and semidetached, in *a* and *b*, respectively) and for the occultation case (*c*). Also shown are the inner and outer Lagrangian surfaces, and the resulting dimensions and scale of the system.

simplex-code and in DC was adjusted along with the other variable parameters. The parameter is labeled $\Delta\phi$ in Tables 5 and 6.

Some of the work was modeled with the inclusion of a star spot, which was adjusted automatically by the program. The spot was assumed to be on the cooler component and to be cooler than the surrounding photosphere; a cooler spot placed on the hotter component did not produce as a good a fit. The use of a hotter spot was not attempted in these series of trials. The initial spot parameters were enlightened estimates and were subsequently adjusted. Following previous usage (Milone et al. 1987, 1991), the parameters are: ϕ, the "latitude," although our referee noted correctly that this quantity is actually a polar distance, measured from the pole facing the observer at phase 0; λ is the "longitude," measured clockwise from the line joining star centers, when the system is envisaged to revolve counterclockwise; ρ the spot radius, and t_f, the "temperature factor," which when multiplied by the temperature of the unperturbed photosphere, gives the spot temperature.

As for NH 31, we ran DC first to check the self-consistency of the input data, and then began the SWD runs, starting at the adjusted DC values. The most significant trials are identified below and the parameters resulting from them are listed in Table 5.

Solution set S1 was the result with all weights for the very sparse B light curve set equal to zero, and assuming a detached configuration ($\Omega_1 \neq \Omega_2$);

S2 is the result of restarting the simplex at S1 but with B data included and assuming the contact configuration ($\Omega_1 = \Omega_2$);

S3 is the solution with the same data set and beginning simplex as S2 but now assuming a dark spot on component 2. The spot parameters were kept fixed at values

$$\phi = 90°, \quad \lambda = 53\overset{\circ}{.}0, \quad \rho = 54\overset{\circ}{.}0, \quad t_f = 0.70,$$

where ϕ, λ, ρ, and t_f are the spot parameters defined earlier;

S4, as per S3 but spot parameters fitted; $L_1(B)$ found too small; spot parameters permitted range too small;

S5, as per S4, but with larger spot parameter ranges and $L_1(B)$ manually adjusted. The final spot parameters were

$$\phi = 71\overset{\circ}{.}04, \quad \lambda = 70\overset{\circ}{.}45, \quad \rho = 53\overset{\circ}{.}90, \quad t_f = 0.829.$$

The WD solution starting at S5 is contained in Table 6, and the observed and computed light curves are shown in Figure 3*a*. The fit is seen to be satisfactory, except for the scattered points suggestive of a variable O'Connell effect at maximum I ($\phi \approx 0.25$). The x-z plane cross section of the system with these parameters is shown in Figure 4*a*. It is interesting that the system appears to be overcontact and very close to its outer Lagrangian surface. This is hardly a broken-contact condition. The preference for $\imath \approx 75°$ indicates partial eclipses, so that the mass ratio cannot be considered secure (see Milone et al. 1991), until confirmed by spectroscopy, also required for T_1 and M_1, and M_2.

The adopted solution is for light curves which were weighted more heavily in the minima. The constraints imposed on this solution were again probed with a series of DC runs for which the weights of all data points were set equal. These results are shown in the second ("unweighted") column of DC solutions of Table 6. As we noted for the NH 31 system, the quantity Σwr^2 for the new run cannot be compared to the adopted solution result. The parameters are not changed, so the adopted ("weighted") solution effectively survives this test.

5. NH 30

NH 30 also shows an O'Connell effect and a depth difference of $\sim$0.10 mag. It is demonstrated to be a constant system also.

TABLE 5

NH 19 SIMPLEX-DERIVED PARAMETERS

Parameter	S1	S2	S3	S4	S5
Mode	3	3	3	3	3
i	75°.16	75°.22	75°.08	75°.07	75°.00
Ω_1	2.506	2.482	2.490	2.483	2.586
Ω_2	2.545	2.482	2.490	2.483	2.586
$\Delta\phi$	0.0022	0.0057	0.0012	0.0025	0.0019
q	0.425	0.411	0.440	0.432	0.495
T_2 (K)	7013	7006	7486	7261	7311
$L_1(V)(4\pi)$	7.01	7.04	6.88	7.12	6.92
$L_1(B)(4\pi)$	...	8.25	7.49	7.70	8.20
σ	±0.035	±0.036	±0.030	±0.031	±0.029
N	86	150	150	150	150

TABLE 6

NH 19 FINAL DC PARAMETERS

Parameter	S6 (unequal weight)	S6 (equal weight)
i	74°.12 ± 1°.01	74°.12 ± 1°.34
$\Omega_1 = \Omega_2$	2.586 ± 0.069	2.586 ± 0.079
q	0.495 ± 0.040	0.485 ± 0.041
T_2 (K)	7311 ± 150	7311 ± 98
$L_1(V)(4\pi)$	6.913 ± 0.081	6.913 ± 0.122
$L_1(B)(4\pi)$	7.958 ± 0.165	7.958 ± 0.192
$L_2(V)(4\pi)$	2.591	2.541
$L_2(B)(4\pi)$	2.663	2.606
R_1/a (pole)	0.468 ± 0.022	0.465 ± 0.024
R_1/a (side)	0.513 ± 0.034	0.510 ± 0.037
R_1/a (back)	0.574 ± 0.065	0.567 ± 0.068
R_2/a (pole)	0.356 ± 0.018	0.350 ± 0.019
R_2/a (side)	0.384 ± 0.026	0.377 ± 0.027
R_2/a (back)	0.516 ± 0.202	0.491 ± 0.149
Σwr^2	2.554	0.955
σ	0.0284	0.0338

A large number of SWD trials resulted in the more significant solution sets listed in Table 7. The large range in q indicates that this parameter was not well determined. For all trials, $T_1 = 8130$ K was assumed. The solution sets are identified as follows:

S1.—initial simplex as per DC trial; *B* light curve omitted;

S2.—starting with S2, but *B* light curve included;

S3.—starting with S2, but with adjustable spot on star 2, yielding parameters

$$\phi = 90°.22, \quad \lambda = 99°.22, \quad \rho = 11°.23, \quad t_f = 0.71;$$

S4.—starting with S3, but fixing $i = 90°$, yielding

$$\phi = 100°.50, \quad \lambda = 116°.25, \quad \rho = 11°.50, \quad t_f = 0.72;$$

S5.—starting with S4, and permitting larger variation in spot parameters, resulting in nearly black spots

$$\phi = 140°.62, \quad \lambda = 173°.46, \quad \rho = 27°.18, \quad t_f = 0.01;$$

S6.—starting with S1, but with adjustable spot on star 2, yielding parameters

$$\phi = 132°.18, \quad \lambda = 8°.29, \quad \rho = 36°.79, \quad t_f = 0.68.$$

S7.—starting with DC-adjusted solution (which started from S6); spots retained at final S6 values.

The constraints on the ranges of the inclination, the spot parameters, and on T_2 are particularly weak. Solutions 2–5 have a common, fatal flaw in that they yield models which *exceed* the outer Lagrangian surface and therefore cannot be considered realistic. The rapid dissipation of the system is an event most unlikely to occur at any time, perhaps least of all, in this ancient cluster, the age of which was determined by Nemec & Harris (1987) to be 18 Gy on the basis of the isochrones of VandenBerg & Bell (1985). Solutions S6 and S7 are contained within the outer Roche lobe and are therefore favored. As was true for NH 19, NH 30 is seen to be an overcontact system. Figure 3*b* show the light curves and model S7. Table 8 lists the parameters for the final DC runs. "S6" of Table 8 (DC parameters) represents an adjusted version of "S6" in Table 7 (simplex table). Note that T_2 has shifted from the SWD determination. Accordingly, the SWD run S7 was performed starting with the final DC parameters of S6. The S7 SWD results were then input to DC and the errors determined as the S7 (original) column of Table 8 indicates. "S7" of Table 8 represents a further DC-adjusted solution. This solution also incorporates a different hot spot on star 2 to better fit maximum I where an enhancement amid larger scatter is visible. The system parameters were not significantly changed

TABLE 7

NH 30 SIMPLEX-DERIVED PARAMETERS

Parameter	S1	S2	S3	S4	S5	S6	S7
Mode	3	3	3	3	3	3	3
i	89°.91	89°.99	90°.00	90°.00	90°.00	89°.98	84°.42
$\Omega_1 = \Omega_2$	2.451	2.436	2.026	2.051	2.104	2.401	2.401
q	0.372	0.431	0.237	0.248	0.291	0.353	0.366
T_2 (K)	7023	7158	7769	7648	7008	7522	7302
$L_1(V)(4\pi)$	8.35	8.36	9.42	9.44	9.98	8.21	8.21
$L_1(B)(4\pi)$	...	8.42	9.40	9.72	10.34	8.49	8.49
σ	±0.040	±0.041	±0.042	±0.038	±0.038	±0.039	±0.036
N	65	78	138	150	150	150	150

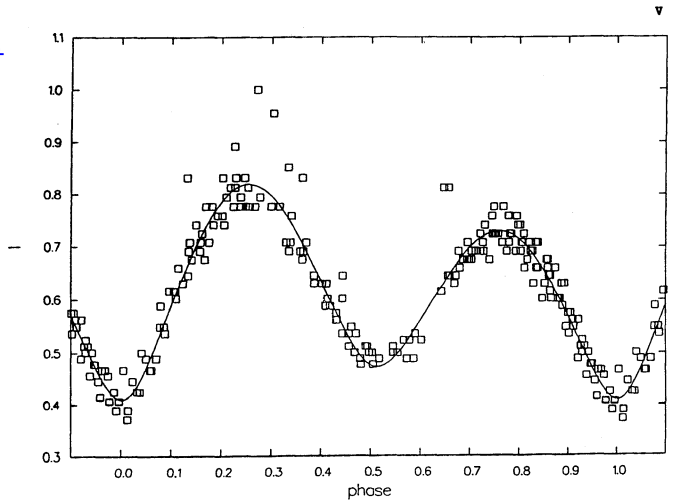

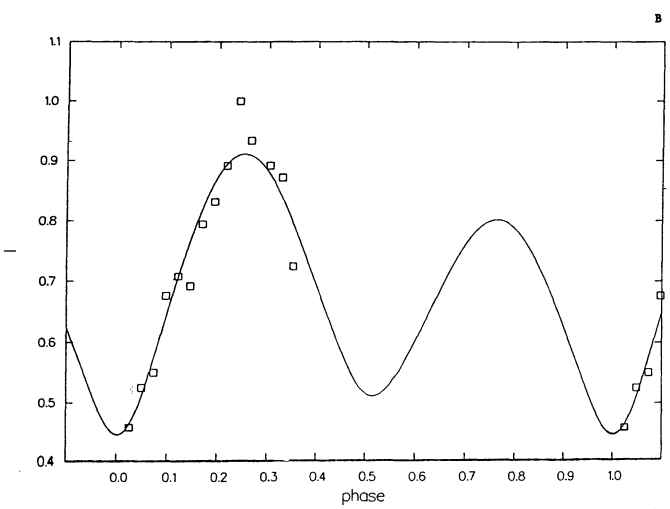

FIG. 3a

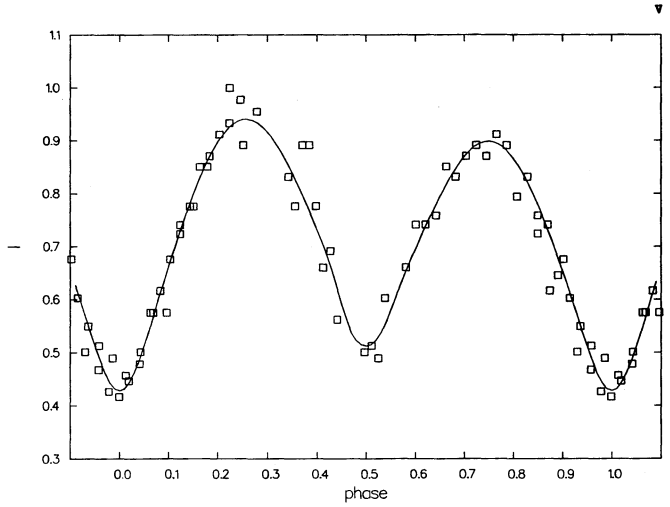

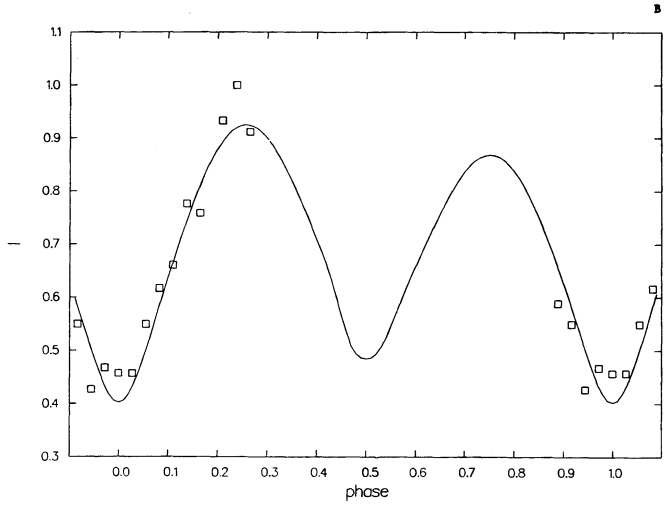

FIG. 3b

FIG. 3.—The observed data and computed V and B light curves of model S6 (Table 6) for the system NH 19 (*a*) and of model S7 (Table 7) for the system NH 30 (*b*) in the globular cluster NGC 5466.

TABLE 8

NH 30 FINAL DC PARAMETERS

Parameter	S6	S7 (original)	S7 (adopted)	S7 (unweighted)
i	84°.42 ± 4°.30	84°.42 ± 3°.07	83°.13 ± 2°.32	80°.74 ± 5°.57
$\Omega_1 = \Omega_2$	2.401 ± 0.080	2.401 ± 0.080	2.395 ± 0.022	2.395 ± 0.034
q	0.353 ± 0.026	0.366 ± 0.023	0.367 ± 0.001	0.371 ± 0.004
T_2 (K)	7302 ± 136	7302 ± 109	7302 ± 113	7297 ± 265
$L_1(V)(4\pi)$	8.207 ± 0.157	8.207 ± 0.181	8.243 ± 0.157	8.195 ± 0.380
$L_1(B)(4\pi)$	8.492 ± 0.244	8.492 ± 0.254	8.483 ± 0.237	8.187 ± 0.472
$L_2(V)(4\pi)$	2.338	2.459	2.481	2.508
$L_2(B)(4\pi)$	2.173	2.289	2.302	2.260
R_1/a (pole)	0.480 ± 0.023	0.483 ± 0.023	0.484 ± 0.005	0.485 ± 0.007
R_1/a (side)	0.526 ± 0.034	0.530 ± 0.035	0.533 ± 0.007	0.534 ± 0.011
R_1/a (back)	0.570 ± 0.054	0.578 ± 0.056	0.582 ± 0.011	0.585 ± 0.016
R_2/a (pole)	0.314 ± 0.018	0.323 ± 0.016	0.326 ± 0.001	0.328 ± 0.003
R_2/a (side)	0.335 ± 0.025	0.346 ± 0.022	0.349 ± 0.001	0.352 ± 0.004
R_2/a (back)	0.427 ± 0.105	0.462 ± 0.144	0.478 ± 0.010	0.297 ± 0.048
Σwr^2	1.382	1.320	1.306	(0.141)
σ	0.0367	0.0358	0.0356	0.0401

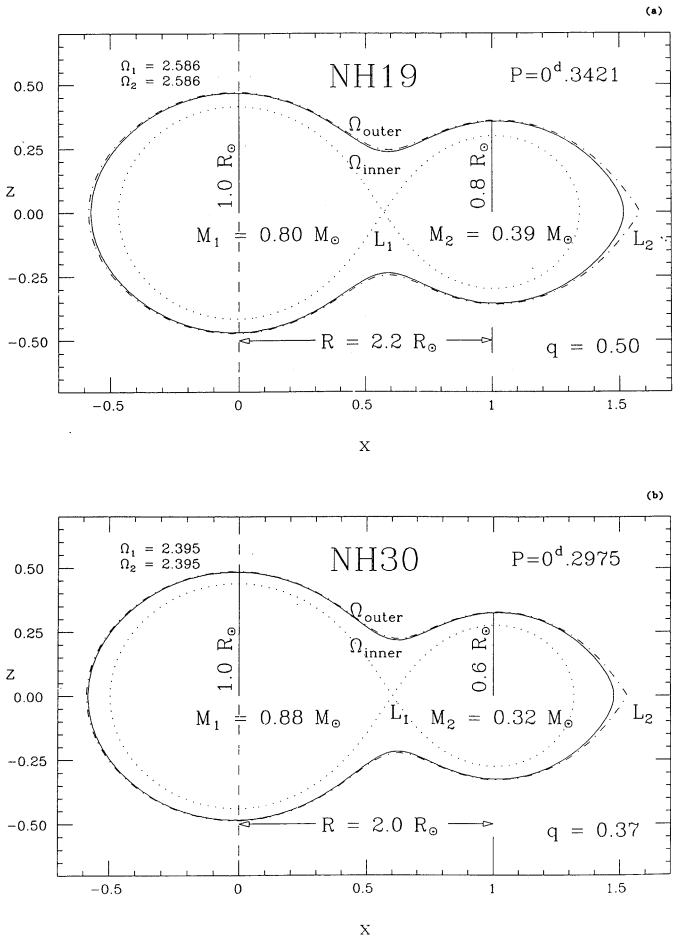

FIG. 4.—The x-z plane profile of the overcontact system NH 19, model S6 of Table 6 (*a*) and of the overcontact system NH 30, model S7 of Table 7 (*b*). Note that the model predicts components very close to the outer Lagrangian surface.

by this addition. The optimized spot parameters were

$$\phi = 80\overset{\circ}{.}00\,, \quad \lambda = 310^\circ\,, \quad \rho = 20\overset{\circ}{.}0\,, \quad t_f = 1.30\,.$$

Even without this substitute spot, the optimized DC and simplex solutions differed slightly for this system. This circumstance reflects primarily the condition that the minima of parameter space are relatively shallow, and secondarily the difference in optimization procedure accorded by both techniques. Looked at in another way, the degree of similarity of the final solutions provides evidence of the degree of robustness of the model. Table 8 suggests that the error in the mass ratio exceeds $\approx 20\%$, but that in L_1 is of order $\approx 4\%$, assuming that the fixed initial values are not greatly in error. The system model was also checked in the DC modeling by adjusting the weights to be equal for all data points across the light curve, as was done for the other systems' solutions. This produced no significant changes in the parameters of the system, although the uncertainty in the parameters increased remarkably. We therefore retain the adopted solution as a sufficiently robust and unique representation of the currently available data of the system. All three final DC solutions are shown in Table 8; the adjusted S7 solution is labeled "adopted." Figure 4*b* shows the x-z plane cut of the system according to model S7 of the simplex runs.

6. SUMMARY AND DISCUSSION

All three systems were modeled with the enhanced DC program of Wilson-Devinney described by Milone et al. (1991). The system solutions do not differ greatly from the preliminary analyses given by Mateo et al., but certain differences, principally with respect to the relative temperatures of the cooler components, have been obtained. In particular, values for T_2 in the W UMa systems NH 19 and NH 30 were assumed by Mateo et al. to be the same as T_1, despite the difference in depth between the minima.

The results of our explorations of the parameter space of the short-period Algol system NH 31 indicate that this system is probably semidetached, and that the inclination must be very close to 90°. However, whether it is detached or semidetached, both stars nearly fill their inner Roche lobes. Under present assumptions, the transit case is slightly preferable to the occultation case. An exploration of the parameter space under the constraint that $q > 1$, suggests that more observations at secondary minimum are required to help decide the case. The secondary minimum of NH 31 is seen to be relatively deep (0.15 mag compared to 0.33 mag for the primary) for an Algol and our solution confirms that the system should be easily resolvable as a double-lined spectroscopic binary, whichever case holds. These data will resolve the question, when they become available.

The modeling of both NH 19 and NH 30 required the use of spots because of the large O'Connell effect (asymmetry at maximum light) in their light curves. All analyses indicate that NH 19 and NH 30 are indeed contact systems, with sizable filling factors. In binary star modeling parlance, they are *overcontact* systems. While the mass ratio, q is well determined from the light curve analyses alone, experience suggests that photometric and spectroscopic mass ratios do not necessarily agree (see, for example, Van Hamme & Wilson 1985), and should be independently checked. Indeed, even though solutions have been explored across great ranges of parameter constraints in this study, we have demonstrated elsewhere that radial velocity curves are important for removing modeling ambiguities in partial eclipse contact binary cases (Milone, Hrivnak, & Wilson 1987; Milone et al. 1991). It is interesting that both contact systems are well fitted under the condition that $q < 1$, i.e., for A-type W UMa stars, and are overcontact. Improved B light curves and spectroscopic data will permit still more precise modeling constraints, but in the context of current theory, the contact systems appear to be in the process of merging through angular momentum loss, possibly by magnetic braking. Continued photometry of these objects is being pursued by Harris & Olszewski at their respective institutions, and by Milone, Schiller, & McVean at Mount Laguna, and this should further improve modeling precision.

Preliminary absolute dimensions of all three systems are given in Table 9. In previous tables, all uncertainties were *probable errors* derived from the covariant matrices; here (and in Table 10), they are *mean standard errors*. The selection of T_1 in each case, based on color indices provided by Mateo et al. (1990), was not altered in the present investigation. Experience indicates that changes of order ≈ 100 K or so in T_1 do not much affect the derived model solution (the Wilson-Devinney program effectively computes ΔT, not T_2 in the modes used here). Since the T_1 values were unchanged, we also assumed the bolometric corrections of Mateo et al. taken from Schmidt-Kaler's (1982) tables, except for the bolometric correction for

the cooler star in the occultation case. Our derived temperature for this component is 8481 K, and we selected a correction, 0.25, slightly more consistent than the value (0.22) they adopted for this component. The effect of this adoption on the derived luminosity and distance is negligible. Our main contribution in this work may be the range of mass ratios permitted for the various viable models, and the luminosity ratios which are needed if double-line spectroscopy is to be carried out. Mateo et al.'s estimates of q (0.10 ± 0.04 and 0.14 ± 0.04 for NH 19 and NH 30, respectively) were determined from statistical properties of Population I field W UMa stars with relatively undistorted light curves (Rucinski 1974). In the case of RW Com, in particular (Milone et al. 1980, 1985; Milone, Wilson, & Hrivnak 1987), these properties did not prove good predictors of the actual parameters of the system. Moreover, Mateo et al. assumed the radius of the inner contact surface as the radius of each component. The radii obtained by Mateo et al. are given in their Table V (1.26 and 0.45 $R_\odot$ for NH 19; 1.10 and 0.45 $R_\odot$ for NH 30, respectively). The results we cite in Tables 9 and 10 are far less dependent on these assumptions, but we continue to assume the Mateo et al.'s values of T_1, and their total mass estimates: 1.2 $M_\odot$, relatively reliably constrained by color index, abundance, and by evolutionary considerations. At the same time, it is important to note the close proximity of the components of NH 19 and NH 30 to their outer Roche lobes, a condition which suggests that mass loss from the system may have proceeded further. Here again, spectroscopy will have to decide the issue.

As might be expected, the computed distances for the individual systems show discrepancies ($< \approx 2\ \sigma$), when compared to the distance derived by Nemec & Harris (1987).

To explore the consequences of constraining the distance to be $V - M_v = 16.00$, as found by Nemec & Harris (1967), we loosened the constraint $M_1 + M_2 = 1.2\ M_\odot$, and recomputed the values of the absolute parameters of the system with new values of M_1 and a (which is constrained by the period and total mass). The former constraint of 1.2 $M_\odot$ for the total mass is appropriate for a main sequence turnoff mass of ≈ 2–$3\ M_\odot$, desired for reasons we discuss later. The changes in absolute elements propagating from the adoption of new masses are shown in Table 10, which combines our modeling with constraints on M. This table is no more definitive than Table 9, because the uncertainty in the temperatures and therefore the luminosities has not been explored. Nevertheless, it indicates that whereas previously NH 30 appeared to be too distant, it now appears to be grossly undermass. This result demonstrates that despite the model uniqueness tests we have conducted, more data are needed to constrain better the initial parameters; it may, however, also mean that the system is indeed a background system.

Thus we emphasize that temperatures and masses of the component stars are required in order to probe their individual evolutionary status. Some spectroscopic classification observations of these three objects have been obtained (H. Harris 1991, private communication) and we are attempting to obtain radial velocities from which the mass ratio and, with light curve analysis, the masses may be determined and to check on the assumed temperatures of the hotter components. The analyses described here have been carried out with the new atmospheres version of the Wilson-Devinney code, both by itself and further enhanced with simplex. No significant differences in results were found among sample runs on the SPARCstation, Myrias, Cyber 205, and IBM RS6000 platforms.

TABLE 9

ABSOLUTE PARAMETERS

A. NH 31

ELEMENT	TRANSIT		OCCULTATION
	Detached	Semidetached	DETACHED
$a\,(R_\odot)$[a]	2.85	2.85	2.85
i	90°.0	90°.0	90°.0
q	0.456 ± 0.025	0.273 ± 0.034	1.488 ± 0.071
$M_1\,(M_\odot)$[a]	0.82	0.94	0.48
$M_2\,(M_\odot)$[a]	0.37	0.26	0.71
$\log \langle g_1 \rangle$	4.33	4.38	4.36
$\log \langle g_2 \rangle$	4.23	4.03	4.26
T_1 (K)	8410	8410	9429
T_2 (K)	7330 ± 128	7309 ± 120	8465 ± 99
$\log (L_1/L_\odot)$	0.67 ± 0.10	0.68 ± 0.10	0.60 ± 0.10
$\log L_2/L_\odot)$	0.19 ± 0.11	0.22 ± 0.11	0.69 ± 0.10
$M_{\rm bol,1}$	3.01 ± 0.25	2.98 ± 0.25	3.18 ± 0.26
$M_{\rm bol,2}$	4.22 ± 0.27	4.13 ± 0.26	2.96 ± 0.26
B.C.$_1$[a]	0.25	0.25	0.35
B.C.$_2$[a]	0.22	0.22	0.22
$M_{v,1}$	2.76 ± 0.25	2.73 ± 0.25	2.83 ± 0.26
$M_{v,2}$	4.00 ± 0.27	3.91 ± 0.26	2.74 ± 0.26
$\langle R_1 \rangle\,(R_\odot)$	1.02 ± 0.12	1.04 ± 0.12	0.75 ± 0.09
$\langle R_2 \rangle\,(R_\odot)$	0.77 ± 0.09	0.81 ± 0.10	1.03 ± 0.12
$(V - M_v)$	16.34 ± 0.20	16.39 ± 0.20	16.77 ± 0.18
Distance (kpc)	18.53 ± 1.69	18.93 ± 1.73	22.57 ± 1.91

B. NH 19 and NH 30

ELEMENT	CONTACT MODE	
	NH 19	NH 30
$a\,(R_\odot)$[a]	2.18	1.99
i	$74°.12 \pm 1°.52$	$83°.13 \pm 2°.32$
q	0.495 ± 0.060	0.367 ± 0.011
$M_1\,(M_\odot)$[a]	0.80	0.88
$M_2\,(M_\odot)$[a]	0.39	0.32
$\log \langle g_1 \rangle$	4.23	4.33
$\log \langle g_2 \rangle$	4.11	4.18
T_1 (K)[a]	8200	8130
T_2 (K)	7311 ± 224	7302 ± 113
$\log (L_1/L_\odot)$	0.71 ± 0.14	0.64 ± 0.10
$\log (L_2/L_\odot)$	0.33 ± 0.27	0.17 ± 0.10
$M_{\rm bol,1}$	2.91 ± 0.35	3.08 ± 0.24
$M_{\rm bol,2}$	3.87 ± 0.70	4.26 ± 0.25
B.C.$_1$[a]	0.24	0.23
B.C.$_2$[a]	0.24	0.23
$M_{v,1}$	2.67 ± 0.35	2.85 ± 0.24
$M_{v,2}$	3.63 ± 0.70	4.03 ± 0.25
$\langle R_1 \rangle\,(R_\odot)$	1.13 ± 0.18	1.06 ± 0.12
$\langle R_2 \rangle\,(R_\odot)$	0.91 ± 0.29	0.77 ± 0.08
$(V - M_v)$	16.11 ± 0.32	16.67 ± 0.19
Distance (kpc)	16.65 ± 2.46	21.54 ± 1.90

[a] Assumed and fixed values. $M_1 + M_2$ constrained to 1.2.

However, the current atmospheres code assumes solar abundances, and in the present modeling case, this assumption is open to attack. The assumption is important, however, only for well-constrained multiwavelength, and especially ultraviolet, flux data. In the present case, the effect on the V light curve modeling results is minimal; the B light curves are sparse and effectively serve only as crude checks on the V pass-band modeling. Certainly, when ultraviolet broad-band or spectrophotometric data become available, appropriate corrections will need to be made for the minimal line blanketing and decreased backwarming effects of these metal-poor stars.

The discovery that these binaries are among the blue stragglers of the cluster, proves the case that at least some, and

TABLE 10

CONSTRAINED ABSOLUTE PARAMETERS

A. NH 31

ELEMENT	TRANSIT		OCCULTATION
	Detached	Semidetached	Detached
$a\,(R_\odot)$	2.44	2.39	2.00
i	90°.0	90°.0	90°.00
q	0.456 ± 0.025	0.273 ± 0.034	1.488 ± 0.071
$M_1\,(M_\odot)$	0.51	0.55	0.17
$M_2\,(M_\odot)$	0.23	0.15	0.25
$\log\langle g_1\rangle$	4.26	4.30	4.21
$\log\langle g_2\rangle$	4.17	3.95	4.11
T_1 (K)	8410	8410	9429
T_2 (K)	7330 ± 128	7309 ± 120	8465 ± 99
$\log(L_1/L_\odot)$	0.54 ± 0.10	0.53 ± 0.10	0.30 ± 0.10
$\log(L_2/L_\odot)$	0.05 ± 0.10	0.07 ± 0.11	0.38 ± 0.10
$M_{\rm bol,1}$	3.35 ± 0.24	3.36 ± 0.25	3.95 ± 0.25
$M_{\rm bol,2}$	4.56 ± 0.26	4.51 ± 0.27	3.73 ± 0.26
B.C.$_1$[a]	0.25	0.25	0.35
B.C.$_2$[a]	0.22	0.22	0.22
$M_{v,1}$	3.10 ± 0.24	3.11 ± 0.25	3.60 ± 0.25
$M_{v,2}$	4.34 ± 0.26	4.29 ± 0.27	3.51 ± 0.26
$\langle R_1\rangle\,(R_\odot)$	0.88 ± 0.10	0.87 ± 0.10	0.53 ± 0.06
$\langle R_2\rangle\,(R_\odot)$	0.66 ± 0.08	0.68 ± 0.08	0.73 ± 0.08
$(V-M_v)$	16.00 ± 0.20	16.00 ± 0.20	16.00 ± 0.18
Distance (kpc)	15.9 ± 1.4	15.9 ± 1.5	15.8 ± 1.3

B. NH 19 and NH 30

ELEMENT	CONTACT MODE	
	NH 19	NH 30
$a\,(R_\odot)$[a]	2.08	1.46
i	74°.12 ± 1°.52	83°.13 ± 2°.32
q	0.495 ± 0.060	0.367 ± 0.011
$M_1\,(M_\odot)$[a]	0.69	0.35
$M_2\,(M_\odot)$[a]	0.34	0.13
$\log\langle g_1\rangle$	4.21	4.19
$\log\langle g_2\rangle$	4.09	4.04
T_1 (K)[a]	8200	8130
T_2 (K)	7311 ± 224	7302 ± 113
$\log(L_1/L_\odot)$	0.67 ± 0.14	0.37 ± 0.13
$\log(L_2/L_\odot)$	0.29 ± 0.28	−0.10 ± 0.13
$M_{\rm bol,1}$	3.01 ± 0.35	3.75 ± 0.33
$M_{\rm bol,2}$	3.97 ± 0.70	4.93 ± 0.34
B.C.$_1$[a]	0.24	0.23
B.C.$_2$[a]	0.24	0.23
$M_{v,1}$	2.77 ± 0.35	3.52 ± 0.33
$M_{v,2}$	3.73 ± 0.70	4.70 ± 0.34
$\langle R_1\rangle\,(R_\odot)$	1.08 ± 0.17	0.78 ± 0.12
$\langle R_2\rangle\,(R_\odot)$	0.87 ± 0.27	0.56 ± 0.08
$(V-M_v)$	16.01 ± 0.32	16.00 ± 0.26
Distance (kpc)	15.9 ± 2.3	15.8 ± 1.9

[a] Assumed and fixed values. Distance constrained.

strengthens the view that many, are products of binary star system evolution, at some stage of a merger process. Mateo et al. argue that the merger mechanism should function only in relatively old clusters, where the turn-off mass is less than ~2 or 3 $M_\odot$, because, according to Iben & Tutukov (1984), this is the upper mass limit for strong magnetic fields which are needed to provide the magnetic braking mechanism for angular momentum loss. The presence of the O'Connell effect in two of the three systems studied here certainly is not at variance with that view, because surface brightness variation across the disk of a component due to stellar active regions is a possible mechanism for the origin of the O'Connell effect. The O'Connell effect has been seen in other A-type systems, and spottedness has been proposed for such systems as well, even though the earlier spectral type of such systems would seem to preclude such phenomena. We can offer no explanation for why stars with assumed radiative envelopes appear to undergo phenomena usually associated with convective envelope stars, nor for the apparent temperature difference between the components of the contact systems (a common phenomenon) but this does seem to be the case.

Mateo et al. predict that between 3% and 15% of all Population II blue stragglers should be *detectable* contact binaries; this is an easy hypothesis to check because blue stragglers are relatively bright and short-period variation is detectable single-night multiple frame CCD surveys of globular clusters. Several investigators, including Milone and Schiller, are already involved in such searches for short-period binaries in clusters. While the evolutionary merger process can certainly yield blue straggler-like products, it is also true that mergers can be greatly aided if not accomplished through binary-binary collisions (because the cross section of such collisions goes as the semimajor axis rather than as the stellar radius as in single star collisions), a process facilitated by the high central density in NGC 5466. Finally, it is possible that blue stragglers can be formed in ways other than through binary mergers (see Leonard 1989, for example, for fuller discussions of both topics).

It is a pleasure to thank Hugh Harris, Al Linnell, Caty Pilachowski, Taft Armandrof, and S. R. Sreenivasan for helpful discussions with E. F. M. Our anonymous referee provided several useful suggestions. This work was supported by an NSERC operating grant and a University of Calgary Research Grant to E. F. M., a University of Calgary Research Fellowship to C. R. S., and a joint Germany-Canada travel grant to H. J. Fahr of the University of Bonn and the University of Calgary from the International Bureau of GKSS Forschungzentrum Geesthacht GMBH, administered by H. Bianchi, for which we are most grateful.

REFERENCES

Breinhorst, R. A., Kallrath, J., & Kämper, B. C. 1989, MNRAS, 241, 559
Drechsel, H., Lorenz, R., & Mayer, P. 1989, A&A, 221, 49
Eggen, O., & Iben, I., Jr. 1989, AJ, 97, 431
Guinan, E., & Bradstreet, D. H. 1988, in Formation and Evolution of Low-Mass Stars, ed. A. K. Dupree & M. T. Lago (Dordrecht: Reidel), 345
Iben, I., Jr., & Tutukov, A. V. 1984, ApJ, 284, 719
Kallrath, J. 1987, Diploma thesis (Bonn: Sternwarte der Universität Bonn)
———. 1992, in Modeling of Eclipsing Binary Stars, ed. E. F. Milone (New York: Springer), in preparation
Kallrath, J., & Linnell, A. P. 1987, ApJ, 313, 346
Leonard, P. J. T. 1989, AJ, 98, 217
Mateo, M., Harris, H. C., Nemec, J., & Olszewski, E. W. 1990, AJ, 100, 469
Milone, E. F., Chia, T. T., Castle, K. G., Robb, R. M., & Merrill, J. E. 1980, ApJS, 43, 339
Milone, E. F., Groisman, G., Fry, D. J. I. F., & Bradstreet, D. H. 1991, ApJ, 370, 677
Milone, E. F., Hrivnak, B. J., Hill, G., & Fisher, W. A. 1985, AJ, 90, 109
Milone, E. F., Hrivnak, B. J., & Wilson, R. E. 1987, ApJ, 319, 325
Milone, E. F., & Schiller, S. J. 1988, in The Extragalactic Distance Scale, ed. S. van den Bergh & C. J. Pritchet (Provo: BYU Press), 182
———. 1991, in The Formation and Evolution of Star Clusters, ed. K. Janes (Provo: BYU Press), 427
Milone, E. F., Stagg, C. R., & Kurucz, R. 1992, ApJ, 379, 123
Milone, E. F., Stagg, C. R., Sugars, B. J. A., McVean, J. R., Schiller, S. J., & Kallrath, J. 1992, in preparation
Mochnacki, S. W. 1981, ApJ, 245, 650
Nelson, R. H., Milone, E. F., Penfold, J. E., & Stagg, C. R. 1992, in preparation
Nemec, J., & Harris, H. C. 1987, ApJ, 316, 172

Rahunen, T. 1982, A&A, 102, 81
Schiller, S. J., & Milone, E. F. 1988, AJ, 95, 1466
Schiller, S. J., Milone, E. F., & Stagg, C. R. 1992, in preparation
Schmidt-Kaler, Th. 1982, in Zahlenwerte und Funktionen aus Naturwissenschaften und Technik, ed. N. Landolt & R. Börnstein (Berlin: Springer), 2b, p. 1
Stagg, C. R., & Milone, E. F. 1992, in Modeling of Eclipsing Binary Stars, ed. E. F. Milone (New York: Springer), in press
VandenBerg, D. A., & Bell, R. A. 1985, ApJS, 58, 561
Van Hamme, W., & Wilson, R. E. 1985, A&A, 152, 25
Wade, R. A., & Rucinski, S. M. 1985, A&AS, 60, 471
Walker, R. L., & Chambliss, C. R. 1990, AJ, 100, 233
Webbink, R. 1976, ApJ, 209, 829